JOURNAL OF SOLID STATE CHEMISTRY 47, 210–218 (1983)

Crystal Chemistry, Magnetic, and Electrical Properties of Hexagonal Plutonium Oxide Chalcogenides: Pu_2O_2X, X = O, S, Se

J. M. COSTANTINI AND D. DAMIEN

DECPu-SEFCAE, CEN, BP 6, 92260 Fontenay-aux-Roses, France

C. H. DE NOVION

DECPu-SESI, CEN, BP 6, 92260 Fontenay-aux-Roses, France

A. BLAISE

DRF/SPhS, CEN-G, 85-X, 38041 Grenoble Cedex, France

AND A. COUSSON, H. ABAZLI, M. PAGÈS

Institut du Radium, 11 Rue Pierre et Marie Curie—75321 Paris Cedex 05, France

Received April 27, 1982; in revised form August 6, 1982

A study was made of the influence of the chalcogen X on the magnetic and electrical properties of Pu_2O_2X (X = O, S, Se) compounds and on bonding in these hexagonal compounds, isostructural with the corresponding rare-earth compounds. The comparison of the cell volumes of Nd_2O_2X and Pu_2O_2X compounds showed that the Pu^{3+} crystal radius decreased from β-Pu_2O_3 to Pu_2O_2Se as "5*f* delocalization" and 5*f*–*p* overlap increased. These plutonium compounds were all found to be antiferromagnetic. This was caused by superexchange coupling interactions via *p* orbitals of the oxygen and chalcogen ions. The Néel temperature increased from β-Pu_2O_3 (26 K) to Pu_2O_2S (28 K) then to Pu_2O_2Se (34 K) showing that 5*f*–*p* covalency was enhanced as the chalcogen electronegativity decreased and the *p* radial extent increased. The hexagonal β-Pu_2O_3 was found to be an insulator while both other compounds were semiconductors with gaps around 0.5 eV. These gaps were interpreted as the energy separation between the 6*d*–7*s* conduction band and the *np* band of the chalcogen X with some overlap of the occupied 5*f* states and the *np* band. A simple electron band scheme of these compounds is proposed on such assumptions.

Nous avons étudié l'influence de l'élément chalcogène X sur les propriétés magnétiques et électriques des oxychalcogénures Pu_2O_2X (X = O, S, Se) ainsi que sur la liaison chimique dans ces composés hexagonaux, isostructuraux des composés similaires de terres rares. En comparant les volumes de maille de Pu_2O_2X et de Nd_2O_2X, on montre que le rayon cristallin de Pu décroit de Pu_2O_3 à Pu_2O_2Se avec l'augmentation des recouvrements 5*f*–*p* et de la "délocalisation" des électrons 5*f*. Ces composés sont tous antiferromagnétiques, la température de Néel augmentant de Pu_2O_3 (26 K) à Pu_2O_2Se (34 K). Cela montre que, lorsque l'électronégativité de X diminue, les interactions de superéchange à travers O^{2-} et X^{2-} se renforcent ainsi que la covalence 5*f*–*p*. Pu_2O_3 hexagonal est isolant alors que les deux autres composés sont semiconducteurs avec un gap voisin de 0,5 eV. Nous avons considéré ce gap comme la différence d'énergie entre la bande de conduction 7*s*–6*d* et la bande *np* du chalcogène X. Les états 5f occupés sont situés juste au-dessous de la bande *np* en la recouvrant partiellement. A partir de ces hypothèses nous avons proposé un modèle de bandes simple pour ces composés.

0022-4596/83 $3.00

I. Introduction

The 5*f* electrons in semimetallic compounds are considered to be less "localized" than the 4*f* electrons, either exhibiting a complex narrow band-like behavior or taking part in the bonding, thereby giving rise to some covalent character. In a recent paper (*1*) Damien and de Novion stressed that "5*f* delocalization" depends strongly on two factors:

(1) the actinide–actinide spacing, as evidenced by the Hill plot (*2*);

(2) the nature of the anionic environment.

In this work our aim was to contribute to a better understanding of the anion environment factor by studying the influence of chalcogen X on bonding in the plutonium oxide chalcogenides Pu_2O_2X. Our choice for these compounds followed three criteria:

(1) Pu–Pu distances are sufficiently large ($\gtrsim$3.6 Å) to rule out any direct *f*–*f* coupling.

(2) In the Pu_2O_2X compounds, as in the isostructural rare-earth hexagonal compounds $(RE)_2O_2X$, the metal should be trivalent.

(3) The $(RE)_2O_2X$ compounds have already been studied thoroughly on structural, optical and magnetic standpoints (*3*, *4*), so they should be a good reference for well localized *f* electrons in this particular crystal symmetry and anion environment.

II. Experimental

Pu_2O_2S and Pu_2O_2Se were prepared by heating mixtures of stoichiometric amounts of PuO_2, Pu hydride and appropriate chalcogen according to the reaction

$$PuO_2 + X + PuH_y (2 < y < 3) \rightarrow Pu_2O_2X + (y/2)H_2 \qquad X = S, Se.$$

Both reactions were carried out at 800°C in silica tubes sealed under high vacuum. The amount of hydrogen evolved in the reaction, from one gram maximum of hydride, was small enough to prevent any hazard of rupture of the sealed tubes.

β-Pu_2O_3 was obtained by reacting stoichiometric amounts of Pu hydride with PuO_2 according to the reaction

$$3PuO_2 + PuH_y (2 < y < 3) \rightarrow 2\beta\text{-}Pu_2O_3 + (y/2)H_2.$$

This reaction was done at about 1250°C in a tungsten crucible heated by an induction furnace. The hexagonal β phase was then quenched by switching off the hf current. More details on this work are available in (*5*). These three compounds are black colored. They were X rayed using a 114.6 mm diameter Norelco camera and the Cu$K\alpha$ radiation. Film dilatation corrections were performed.

The magnetic susceptibilities of powdered samples were measured with the Faraday method from 4 to 300 K at 6 kG, the samples being encapsulated in ultrapure aluminium containers. Preliminary measurements at varying applied fields were performed at room temperature to check that the sample was free from magnetic impurities (*5*).

The electrical resistivities were also measured in the same temperature range using the 4-point method on pelletized samples sealed in copper containers. The pellets were sintered at about 1200°C, except β-Pu_2O_3, to avoid any phase transformation in the sesquioxide (*5*).

III. Results

X-Ray Data

The X-ray powder patterns are indexed in the hexagonal system (see Table I) except two weak extra lines which were at-

TABLE I

X-RAY POWDER PATTERNS OF Pu_2O_2S AND Pu_2O_2Se

Pu_2O_2S a = 3.929(1) Å, c = 6.804(2) Å; z = 0.290, z' = 0.640[a]					Pu_2O_2Se a = 3.962(1) Å, c = 6.986(1) Å; z = 0.290, z' = 0.640[a]				
	2θ		I			2θ		I	
hkl	Observed	Calculated[b]	Observed[c]	Calculated[d]	hkl	Observed	Calculated[b]	Observed[c]	Calculated[d]
001	13.04	13.21	vw	3	002	25.52	25.48	vw	8
100	26.27	26.38	s	14	100	26.04	25.95	vw	3
102		26.39		17	101	28.98	28.98	vs	100
101	29.42	29.54	vs	100	102	36.71	36.70	s	47
102	37.50	37.57	s	35	003	38.63	38.65	vw	10
003	39.92	39.93	w	8	110	45.77	45.79	s	33
110	46.20	46.39	s	30	103	47.14	47.15	s	14
111	48.42	48.39	s	0.8	004	52.28	52.37	vw	2
103		48.40		18	112	53.14	53.14	m	7
200		54.06		2	201	55.13	55.11	m	17
112	53.97	54.06	s	16	104	59.25	59.36	m	8
004		54.08		2	202	60.03	60.07	m	11
201	55.72	55.86	s	17	113	61.38	61.43	m	16
202	61.06	61.04	ms	9	203	67.71	67.84	w	5
104		61.05		10	114	72.07	72.08	w	6
113	62.67	62.71	m	12	210	72.98	72.93	w	0.4
203	68.89	69.16	vw	6	105		73.11		6
005	69.14	69.17	ms	2	211	74.29	74.39	m	14
210	73.84	73.80	m	2	204	78.02	78.07	vw	4
114		73.82		4	212	78.67	78.69	w	10
211	75.33	75.33	s	15	300	84.77	84.75	m	6
105		75.35		5	115		84.92		3
212	79.84	79.85	m	8	213	85.74	85.74	m	6
204		79.86		5	106	88.67	88.70	vw	5
300	85.61	85.77	vw	5	205	91.33	90.71	vw	4
006		85.80		<0.1	214	95.47	95.52	vw	5
301		87.24		0.2	303	97.30	97.33	vw	5
213	87.32	87.25	m	8	220	102.19	102.20	vw	4
115		87.26		5	206	106.31	106.28	vw	4
302	91.51	91.65	w	4	310	108.46	108.20	w	0.2
106		91.68		6	215		108.38		7
205	93.41	93.13	vw	3	222		107.99		2
214	97.54	97.55	vw	7	311	109.69	109.68	w	8
220	103.47	103.51	vw	4	223	115.47	115.50	vw	5
116		103.54		<0.1	313	122.19	122.11	vw	5
310	109.69	109.64	m	1	305	121.13	121.15	vw	1
222		109.64		3	117	119.78	119.73	w	8
304		109.65		3	216	125.66	125.68	w	10
206		109.67		5	207	126.82	126.65	vw	<0.01
311	111.14	111.20	m	9	224		126.95		4
215		111.22		6	401	129.79	129.77	vw	5
107		111.25		1	108	131.29	131.24	vw	6

TABLE I—*Continued*

Pu_2O_2S a = 3.929(1) Å, c = 6.804(2) Å; z = 0.290, z' = 0.640[a]					Pu_2O_2Se a = 3.962(1) Å, c = 6.986(1) Å; z = 0.290, z' = 0.640[a]				
	2θ		I			2θ		I	
hkl	Observed	Calculated[b]	Observed[c]	Calculated[d]	*hkl*	Observed	Calculated[b]	Observed[c]	Calculated[d]
312	116.12	116.01	w	6	314	134.60	134.59	w	7
223	117.80	117.06	w	5	225	145.35	145.11	vw	4
313		124.51		7	320	157.00	156.68	m	0.7
305	124.70	124.53	s	5	315		157.11		18
117		124.55		8	321	160.35	160.50	s	27
400		130.03		0.6	208	164.12	164.20	m	17
224	130.69	130.05	m	3					
216		130.07		13					
008		130.10		0.1					
402		138.21		4					
314	138.62	138.23	ms	10					
108		138.29		7					
403	150.89	150.88	m	6					
225		150.91		9					
321		167.38		45					
315	167.14	167.47	s	27					
217		167.57		9					

[a] Atomic position parameters of Ce_2O_2S taken from (*10*).

[b] Calculations done with the computer program POWD (*8*).

[c] Legend: vw = very weak, m = medium, ms = medium strong, s = strong, vs = very strong.

[d] Calculations were done with the computer program TENSIT (*23*). Intensities were corrected with the appropriate Lorenz polarization factor, but neither absorption coefficient nor temperature factor were taken into account. Space group $P\bar{3}m1$ was assumed as in Ce_2O_2S (see text) (*10*).

TABLE II

LATTICE PARAMETERS (a, c), δ-COEFFICIENT, AND SHORTEST PU–PU DISTANCE d OF Pu_2O_2X COMPOUNDS

	a (Å)		c (Å)		c/a			
	This work	Literature	This work	Literature	This work	Literature	δ (%)	d (Å)
β-Pu_2O_3	3.836 (2)	3.8388 (2) (*9*)	5.976 (9)	5.9594 (6) (*9*)	1.56	1.56	0.2	~3.75
Pu_2O_2S	3.929 (1)	3.927 (3) (*10*)	6.804 (2)	6.769 (10) (*10*)	1.73	1.72	0.3	~3.65
Pu_2O_2Se[a]	3.962 (1)	3.957 (*11*)	6.986 (1)	6.977 (*11*)	1.76	1.76	0.7	~3.70
	3.961 (1)		6.982 (1)					

[a] 2 preparations.

tributed to PuO_2. Examination of the line intensities suggests that the Pu_2O_2X compounds are isostructural with the rare-earth compounds $(RE)_2O_2X$ of Ce_2O_2S-type structure (*6, 10, 24*) or *A*-type $(RE)_2O_3$ (*7*). The lattice parameters were calculated with the computer program POWD (*8*). As can be seen in Table II, they are in rather good agreement with the previous determinations (*9–11*).

Magnetic Susceptibility Results

The reciprocal molar susceptibilities of the three compounds are plotted against temperature in Fig. 1, the diamagnetic contributions of Pu^{3+}, O^{2-}, and X^{2-} (*12*) as well as the blank value being substracted from the data. In each compound a slight field dependence of the magnetic susceptibility was observed at room temperature and was attributed to small contents of a ferromagnetic impurity. The reported susceptibility data are subsequently corrected with the aid of the Honda–Owen treatment (*13*).

The maximum in susceptibility is attributed to antiferromagnetic ordering occuring at 26 K for β-Pu_2O_3, 28 K for Pu_2O_2S, and 34 K for Pu_2O_2Se. For β-Pu_2O_3 McCart *et al.* (*14*) found a susceptibility maximum at 20 K while Flotow and Tetenbaum observed a λ-type specific heat anomaly at 17.6 K (*16*). The former authors (*14*) associated this Néel temperature with the maximum value of $d\chi/dT$.

The higher temperature data, between 100 and 300 K, are analyzed with the Curie–Weiss law. The effective moments per Pu atom (p), the Curie paramagnetic temperatures (θ_p), and the Néel points (T_N) are reported in Table III. These p values are higher than the standard free ion value of Pu^{3+} ($\sim 1.23\mu_B$ (*16*)). These differences are not well understood. The high values of θ_p compared to T_N suggest that strong interactions might exist between paramagnetic moments. The analysis of the paramagnetic region requires a more sophisticated treatment needing spectroscopic data on the ground level splitting, and susceptibility data at much higher temperatures.

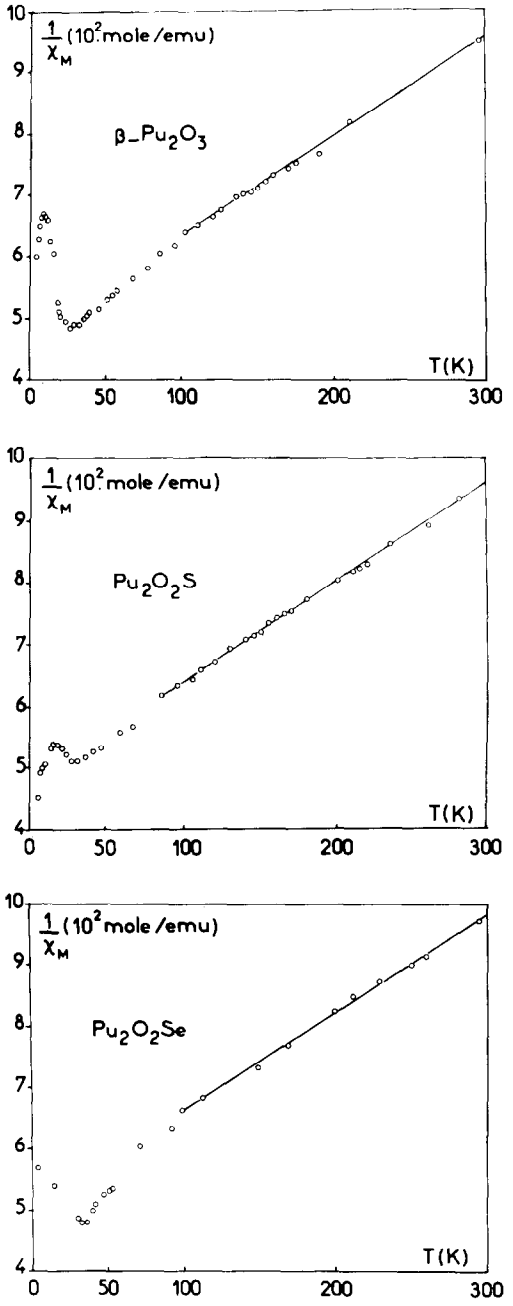

FIG. 1. Thermal dependence of the reciprocal molar susceptibility of β-Pu_2O_3, Pu_2O_2S, and Pu_2O_2Se.

Electrical Resistivity Results

β-Pu_2O_3 was found to be an insulator with $\rho \sim 10^8$ Ω cm at room temperature, while both other compounds are semiconductors with high resistivity $\rho \sim 10^4$ Ω cm at room temperature. This emphasizes the evolution of an ionic compound (β-Pu_2O_3) to covalent compounds (Pu_2O_2S and Pu_2O_2Se).

Below 150 K the resistance of the samples became very high so that we were unable to make reliable measurements at low temperature. Neither time dependent nor temperature hystereses effects were observed.

From the plots of ρ versus $1/T$, given in Fig. 2, activation energies W for electrical conduction were deduced according to the well-known relation $\ln \rho/\rho_0 = W/kT$. Then we calculated a gap $E_g = W/2$, assuming that these compounds are intrinsic semiconductors (see below).

IV. Discussion

Crystal Chemistry

The cell volumes V of these compounds are compared to those of the isostructural Nd_2O_2X compounds (X = O, S, Se). This comparison is justified by the fact that the crystal radii of Nd^{3+} and Pu^{3+} in trihalides are very close (*18*). In the same way, the cell volumes of A–Nd_2O_3 (76.32 Å^3) (*17*) and β-Pu_2O_3 (76.15 Å^3) are nearly equal. Thus we consider that the cell volume of the Nd_2O_2X compounds (*3*) corresponds to the cell volume of an hypothetical compound of Pu^{3+} with localized $5f$ electrons. We then calculate a coefficient δ measuring the relative difference between the cell volumes of the corresponding phases of Nd and Pu. Let us define δ as

$$\delta = 1 - \frac{V(Pu_2O_2X)}{V(Nd_2O_2X)} \qquad \text{with } V = \frac{\sqrt{3}}{2} a^2 c.$$

The increase of δ along the series (see Table II) shows the progressive delocalization of Pu $5f$ electrons from β-Pu_2O_3 to Pu_2O_2Se.

The more $5f$ electrons delocalize with respect to the rare-earth-like situation, the less they shield the nuclear potential. Hence the $6s$ and $6p$ outer shells become more tightly bound and the Pu^{3+} crystal radius shrinks. Thus $5f$ "delocalization" increases from β-Pu_2O_3 to Pu_2O_2Se, while the

TABLE III

MAGNETIC DATA AND GAPS OF Pu_2O_2X COMPOUNDS

X	O	S	Se
T_N (K)	26	28	34
p (μ_B)	1.58	1.58	1.58
θ_p (K)	−300	−300	−320
E_g (eV)	?	0.55	0.54

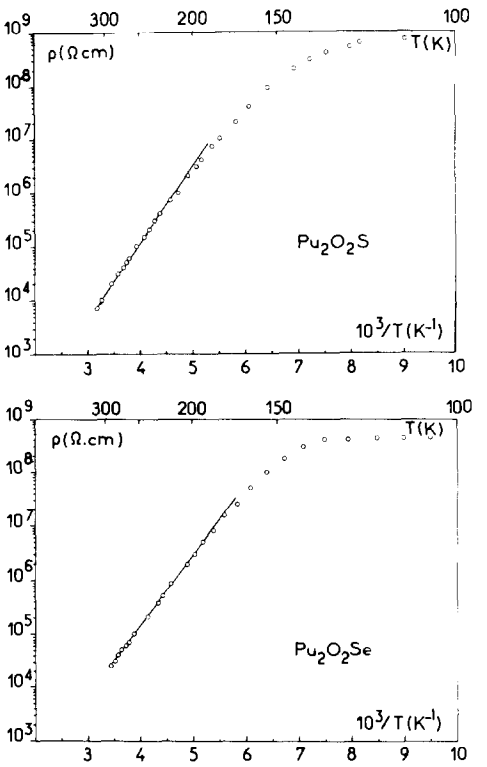

FIG. 2. Plot of the electrical resistivity in log units versus reciprocal temperature for Pu_2O_2S and Pu_2O_2Se.

Pu oxidation state and crystal structure remain the same.

Magnetic Properties

The shortest Pu–Pu distance d has been estimated in each compound (see Table II) using the atomic coordinates of the Nd atoms ($z = 0.245$) in A–Nd_2O_3 (*17*) for β-Pu_2O_3, and of the Ce atoms ($z = 0.290$) in Ce_2O_2S (*10*) for Pu_2O_2S and Pu_2O_2Se; d stands for the metal–metal spacing inside the Pu–O layers (see Fig. 3). It is nearly the same in the three compounds (~3.7 Å), and is shorter than the lattice parameter a, yet it is still longer than the critical distance (~3.4 Å) found in the Hill plot of Pu-based compounds (*2*). This agrees with the localized magnetism found in these compounds.

As the Pu–Pu distances are large enough to rule out a direct f–f exchange coupling, the $5f$ magnetic moments must be coupled via the nonmagnetic p orbitals of the oxygen and chalcogen ions, since here the conduction electrons cannot mediate these interactions. Since T_N increases from β-Pu_2O_3 (26 K) to Pu_2O_2S (29 K) then to Pu_2O_2Se (34 K), we conclude that the superexchange interactions are enhanced with decreasing electronegativity of the chalcogen X and increasing p radial extent. Hence the $5f$ contribution to bonding increases from β-Pu_2O_3 to Pu_2O_2Se. This conclusion from the magnetic data is in agreement with the above-mentioned "delocalization" inferred from crystal chemistry. This effect is small, yet it shows the sensitivity of the $5f$ shell to the anionic ligand field in spite of the shielding of $6s$ and $6p$ outer shells.

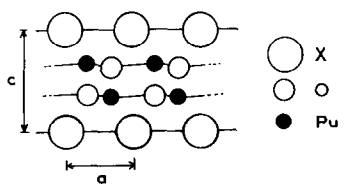

FIG. 3. Layer structure of hexagonal Pu_2O_2X compounds (X = O, S, Se) projected on a {1, 0, 0} plane.

Low temperature specific heat measurements and neutron diffraction experiments on ^{242}Pu-based compounds would certainly be necessary to give the Néel points with better accuracy and determine the magnetic structures, as was done for β-Pu_2O_3 (*14*).

It must be noted that the A-type sesquioxides Ce_2O_3, Pr_2O_3, and Nd_2O_3 do not order above 2 K (*19*); nor do Ce_2O_2S, Ce_2O_2Se, Pr_2O_2S, and Nd_2O_2S (*3, 4*). This is probably due to the smaller radial extent of the more internal $4f$ orbitals, which cannot overlap the neighboring p orbitals.

Electrical Properties

The hexagonal Nd_2O_2X compounds are known to be stoichometric compounds and to have a layered crystal structure (*20*). From a crystallographic standpoint, Nd_2O_2S is made from A–Nd_2O_3 by substituting sulfur sheets for oxygen sheets in between the (Nd–O) layers. Hence we have assumed that Pu_2O_2S and Pu_2O_2Se might be stoichiometric as is β-Pu_2O_3 (*14, 15*). Thus we shall consider here that the measured electrical conductivity of Pu_2O_2S and Pu_2O_2Se has an intrinsic origin. We shall discuss the electrical properties on the basis of a simple band model. This model must account for the fact that β-Pu_2O_3 was found to be an insulator while Pu_2O_2S and Pu_2O_2Se are semiconducting materials.

Let us consider the following three bands (see Fig. 4):

(1) the empty $6d$–$7s$ conduction states of Pu^{3+}

(2) the full $2p$ band arising from the $2p$ states of the oxygen atoms building up the (Pu–O) layers;

(3) the full np bands arising from the chalcogen np orbitals.

The occupied $5f$ states of Pu^{3+} are superimposed on the p valence bands.

Two cases may occur:

(1) If the $5f$ states lie *below* the np band

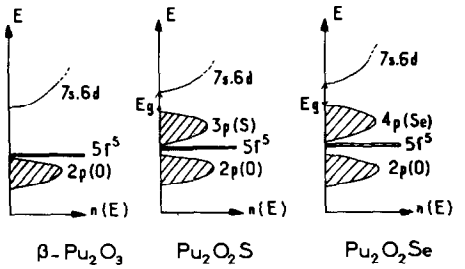

FIG. 4. A schematic band model of hexagonal Pu_2O_2X.

(3*p* for Pu_2O_2S and 4*p* for Pu_2O_2Se), then the measured gap E_g corresponds to an $np \rightarrow 6d-7s$ transition.

(2) If the 5*f* states lie *above* the *np* band then this gap corresponds to a $5f \rightarrow 6d-7s$ transition.

From β-Pu_2O_3 to Pu_2O_2Se, crystal structure remaining unchanged, the crystal field splitting of the 6*d* states must decrease, since the chalcogen electronegativity decreases and the cell volume increases. Thus the bottom of the 6*d* empty states rises from β-Pu_2O_3 to Pu_2O_2S and the conduction band narrows from Pu_2O_2S to Pu_2O_2Se.

The width of the 5*f* states is very slightly affected by this crystal field effect, yet 5*f* states rise a little as covalency increases ("delocalization"). The 3*p* band in Pu_2O_2S and 4*p* band in Pu_2O_2Se are higher in energy than the 2*p* states of oxygen in β-Pu_2O_3, which lie below the 5*f* states (*25*). Hence we are led to think that the appearance of a semiconducting behavior in Pu_2O_2S is due to the 3*p* band which comes closer to the conduction states. Thus we think that E_g represents an $np \rightarrow 6d-7s$ transition. If it had been a $5f \rightarrow 6d-7s$ transition, as was the $4f \rightarrow 5d-6s$ transition in SmS, SmSe, SmTe (*21, 22*), we probably would have observed an *increase* of the gap. Hence in Pu_2O_2S and Pu_2O_2Se, the occupied 5*f* states must lie below the bottom of the chalcogen *np* band. They must also overlap this band to insure the superexchange coupling interactions.

V. Conclusion

We have shown that, in the isostructural compounds β-Pu_2O_3, Pu_2O_2S, and Pu_2O_2Se, the chemical bonding possesses a $5f-p$ covalent character which is enhanced from β-Pu_2O_3 to Pu_2O_2Se. This is due to the increase of the *p* radial extent of the chalcogen ions, and the decrease of electronegativity, from oxygen to selenium. This leads to

(1) a shrinkage of the Pu^{3+} crystal radius,
(2) an increase of the Néel temperature.

We have also pointed out, in Pu_2O_2S and Pu_2O_2Se, that the occupied 5*f* states must overlap the *bottom* of the chalcogen *np* band to account for the electrical properties of this series of compounds. Optical absorption (or reflection) spectra and UPS-valence band spectra would certainly help to improve the understanding of the electronic properties to these compounds.

Acknowledgment

The authors thank Professor Guillaumont for helpful discussions and advice.

References

1. D. DAMIEN AND C. H. DE NOVION, *J. Nucl. Mater.* **100,** 167 (1981).
2. H. H. HILL, *in* "Plutonium 1970" (W. Miner, Ed.), p. 2, Metallurgical Society of AIME, New York (1970).
3. Y. ABBAS, Thèse Grenoble (1976).
4. J. ROSSAT-MIGNOD, Thèse Grenoble (1972).
5. J. M. COSTANTINI, CEA-R- 4056 (1980).
6. J. FLAHAUT, M. GUITTARD, AND M. PATRIE, *Bull. Soc. Chim. Fr.*, 180, p. 990 (1958).
7. E. F. WESTRUM, JR., *in* "Progress in the Science and Technology of Rare Earths," Vol. 1, pp. 310–350, Pergamon, New York (1964).
8. D. E. WILLIAMS, U.S. Atomic Energy Commission Doc. I.S. 105 (1964).
9. E. R. GARDNER, T. L. MARKIN, AND R. S. STREET, *J. Inorg. Nucl. Chem.* **27,** 541 (1965).
10. W. H. ZACHARIASEN, *Acta Cryst.* **2,** 60 (1949).

11. M. ALLBUTT AND A. R. JUNKISON, AERE-R-5541 (1967).
12. L. N. MULAY, *in* "Magnetic Susceptibility," p. 1782, Wiley–Interscience, New York (1966).
13. L. F. BATES, *in* "Modern Magnetism," p. 133, Cambridge Univ. Press, London/New York (1951).
14. B. MC CART, G. H. LANDER, AND A. T. ALDRED, *J. Chem. Phys.* **74,** 5263 (1981).
15. H. E. FLOTOW AND M. TETENBAUM, *J. Chem. Phys.* **74,** 5269 (1981).
16. D. J. LAM AND A. T. ALDRED, *in* "The Actinides, Electronic Structure and Related Properties," Vol. 1, Chap. 3, Academic Press, New York (1974).
17. P. ALDEBERT AND J. P. TRAVERSE, *Mat. Res. Bull.* **14,** 303 (1979).
18. C. KELLER, *in* "The Chemistry of the Transuranium Elements," Vol. 3, p. 125, Verlag Chemie, Weinheim (1971).
19. K. N. R. TAYLOR AND M. I. DARBY, *in* "Physics of Rare Earth Solids," Chapman and Hall, London (1972).
20. P. CARO, *J. Less-Common Met.* **16,** 367 (1968).
21. C. M. VARMA, *Rev. Mod. Phys.* **48,** 219 (1976).
22. A. JAYARAMAN *et al.*, *Phys. Rev. Lett.* **25,** 1430 (1970).
23. D. K. SMITH, U.S. Atomic Energy Document UCRL-7196 (1963).
24. A. BENACERRAF, M. GUITTARD, L. DOMANGE AND J. FLAHAUT, *Bull. Soc. Chim. Fr.* 303, p. 1920 (1959).
25. D. COURTEIX, J. CHAYROUSE, L. HEINTZ, AND R. BAPTIST, *Solid State Comm.* **39,** 209 (1981).